Radiation Treatment Planning: Mixed Integer Programming Formulations and Approaches*

Michael C. Ferris Robert R. Meyer† Warren D'Souza‡

October 2002

Abstract

Radiation therapy is extensively used to treat a wide range of cancers. Due to the increasing complexities of delivery mechanisms, and the improved imaging devices that allow more accurate determination of cancer location, determination of high quality treatment plans via trial-and-error methods is impractical and computer optimization approaches to planning are becoming more critical and more difficult.

We outline three examples of the types of treatment planning problem that can arise in practice and strive to understand the commonalities and differences in these problems. We highlight optimization approaches to the problems, and particularly consider approaches based on mixed integer programming. Details of the mathematical formulations and algorithmic approaches are developed and pointers are given to supporting literature that shows the efficacy of the approaches in practical situations.

1 Introduction

Approximately 1.2 million new cases of cancer are reported each year in the United States, with many times that number occurring worldwide. About 40% of people diagnosed with cancer in the U.S will undergo treatment with radiation therapy. This form of therapy has undergone tremendous

*This material is based on research partially supported by the National Science Foundation Grants ACI-0113051, DMI-0100220, and CCR-9972372 and the Air Force Office of Scientific Research Grant F49620-01-1-0040.

†Computer Sciences Department, University of Wisconsin, 1210 West Dayton Street, Madison, Wisconsin 53706, USA. (ferris,rrm@cs.wisc.edu)

‡Department of Radiation Oncology, University of Maryland School of Medicine, 22 South Green Street, Baltimore, MD 21201 (wdsou001@umaryland.edu)

improvement from a treatment planning standpoint over the last decade, having benefited significantly from advances in imaging technology for computed tomography (CT), magnetic resonance imaging (MRI) and ultrasound (US). As a result of these advances, there has been an increased trend toward image-based radiation therapy treatment planning.

In treatment planning problems, the objective is to deliver a homogeneous (uniform) dose of radiation to the tumor (typically called the target) area while avoiding unnecessary damage to the surrounding tissue and organs. In many cases, near the target there are several structures (typically called organs at risk (OAR)) for which the dose must be severely constrained due to the probability of damage that will lead to medical complications. Since the target and OAR structures can be more accurately identified, the delivery of radiation that accurately conforms to these tissues becomes an achievable goal.

The planning process is determined, not only by the target and the proximal organs at risk, but also by the physical characteristics of the mechanism that will be used to deliver the dose. Teletherapy [5] is the common collective name for the various kinds of external beam radiation treatment, whereas brachytherapy ("brachy" is a Greek prefix implying a short distance) involves the placement of radioactive source configurations near or within the tumor. The availability of additional data and levels of control of radiation delivery procedures adds great complexity to the problem of determining high quality treatment plans.

Classical radiation therapy treatment planning (sometimes called forward planning) was generally a trial and error process in which improved plans were generated by iteratively experimenting with different incident high-energy beam configurations for teletherapy and with alternative placements of sources for brachytherapy. In recent years, there has been a move toward computer generated plans (sometimes termed inverse planning). These planning procedures increase the allowable complexities when the dose is delivered by radioactive implants (brachytherapy), or when the radiation is fired from a number of angles (external beam therapy). Some further extensions include the use of scans in conjunction with the planning procedure, the use of intensity modulation of portions of the beam (termed pencil beams or beamlets), and the use of stereotactic devices to greatly improve the accuracy of the delivered doses of radiation. There are many techniques available to generate treatment plans for each type of radiation delivery system. However, there are definite commonalities arising in all these problems that we shall endeavour to highlight here.

A unified and automated treatment process has several potential benefits

relative to the classical trial-and-error approach. Among these the most important ones are the reduction in planning time and the improvement and uniformity of treatment quality that can be accomplished.

It is usual for the treatment goals to vary from one planner to the next, so a planning tool must be able to accommodate several different goals. Among these goals, the following are typical, although the level of treatment and importance of each may vary.

1. A "homogeneity" goal: An isodose curve is delineated around the volume to ensure delivery of a certain fraction of the maximum delivered dose. A typical homogeneity goal requires that the $x\%$ isodose line encompasses the target volume. Such requirements can be enforced using lower and upper bounds on the dose, or approximated via penalization. (Upper bounds are of lesser importance in brachytherapy since tissues adjacent to the radioactive sources automatically receive high doses.)

2. A "conformity" goal: The overall dosage to the patient is typically limited, and this goal specifies a lower bound on the fraction of that dose to be delivered to the target itself.

3. "Avoidance" goals: These limit the dose delivered to certain sensitive structures (OAR) close to the target.

4. "Simplicity" goals: it is preferable to use as simple a procedure as possible since this reduces "implementation" errors (and frequently reduces treatment time) and allows more patients to be treated with the available resources.

There are often standards established by various professional and advisory groups that specify acceptable homogeneity and conformity requirements.

In all formulations, we need to determine the dose delivered ($Dose$ at a voxel (i, j, k)) from a particular source (e.g. a pencil beam or a radioactive source). A critical feature of all these problem areas is that a functional form for such dose is either highly nonlinear, or is described by a large amount of data that specifies the dose delivered to each voxel of the region of interest. We outline techniques based on both of these approaches.

In a practical setting, many constraints on dose (measured in units called Gray, abbreviated as Gy) are phrased as dose-volume histogram (DVH) constraints of the form:

> no more than 30% of volume X should exceed 10 Gy

or

at least 80% of volume Y should exceed 30 Gy

These constraints are hard to enforce due to the fact that the model needs to determine on a per-voxel basis whether the threshold value is exceeded or not. For example, in the first case, the following constraints could be used

$$\begin{aligned} Dose(i,j,k) &\leq 10 + M * Exceed(i,j,k) \quad \forall (i,j,k) \in X \\ \sum_{(i,j,k)\in X} Exceed(i,j,k) &\leq 0.3 * card(X), \end{aligned}$$

where $Exceed(i,j,k)$ is a binary variable. Standard integer programming issues relating to the choice of the constant M ensue. More generally, when the threshold value is $U_{\mathcal{R}}$ and the percentage limit on overdose in region $\mathcal{R}$ is $\beta_{\mathcal{R}}$ we have

$$\begin{aligned} Dose(i,j,k) &\leq U_{\mathcal{R}} + M * Exceed(i,j,k) \quad \forall (i,j,k) \in \mathcal{R} \\ \sum_{(i,j,k)\in\mathcal{R}} Exceed(i,j,k) &\leq \beta_{\mathcal{R}} * card(\mathcal{R}). \end{aligned} \tag{1}$$

These formulations can become quickly impractical due to large numbers of voxels in the regions of interest. In practice, many modelers use approximate techniques to enforce these constraints. Alternatively, subproblems corresponding to subsets of the region of interest may be sequentially solved.

The conformity of the plan presents even more computational difficulties to a modeler since it involves all voxels receiving radiation. The conformity index C is an estimate of the ratio of the dose delivered to the target, divided by the total dose delivered to the patient. These indices can be used to enforce a conformity requirement using:

$$C \sum_{(i,j,k)} Dose(i,j,k) \leq \sum_{(i,j,k)\in\mathcal{T}} Dose(i,j,k). \tag{2}$$

If conformity is part of the model constraint set, then an appropriate value for C needs to be ascertained beforehand. A reasonable conformity index for a given patient plan is very hard to estimate *a priori* since it depends critically on how complicated the delivery mechanism is allowed to be by the planner and how the volume of the target interacts with the volumes of the allowed delivery.

This paper is not intended to be a complete survey of the use of optimization techniques within treatment planning problems (see [29, 36, 38, 50]

for more complete overviews of conformal radiation therapy, for example). In addition to these survey articles, there are a variety of other approaches (for which we cite representative papers) including those based on optimal control primitives [1], or simulated annealing [27, 32, 43, 44], iterative (relaxation) techniques [10], approaches using biological objectives [7, 24, 33] techniques of multi-objective [22] and neuro-dynamic programming [20]. In this paper we specifically outline three particular problem areas that arise in treatment planning and highlight the discrete nature of some of the decisions that need to be made. Some detail of the underlying applications are given, along with an overview of several solution approaches we feel are promising. This survey is organized as follows: the following two sections describe successful optimization applications to Gamma Knife teletherapy and to brachytherapy for prostate cancer. We then consider extensions of these and related approaches to other teletherapy mechanisms such as IMRT (intensity modulated radiation therapy), and conclude with an assessment of future research directions in radiation treatment planning.

2 Gamma Knife Radiosurgery

The Gamma Knife is a highly specialized treatment unit that provides an advanced stereotactic approach to the treatment of tumor and vascular malformations within the head [21]. The Gamma Knife (see Figure 1(a)) delivers a single, high dose of radiation emanating from 201 Cobalt-60 unit sources. All 201 beams simultaneously intersect at the same location in space to form an approximately spherical dose region that is typically termed a shot of radiation. A typical treatment consists of a number of shots, of possibly different sizes and different intensities, centered at different locations in the tumor, whose cumulative effect is to deliver a certain dose to the treatment volume while minimizing the effect on surrounding tissue.

Gamma Knife radiosurgery begins (after administering local anesthesia) by fixing a stereotactic coordinate head frame to the patient's head using adjustable posts and fixation screws. This frame establishes a coordinate system within which the target location is known precisely and also serves to immobilize the patient's head within an attached focusing helmet during the treatment (see Figure 1(b)). An MRI or CT scan is used to determine the position of the treatment volume in relation to the coordinates determined by the head frame. Once the location and the volume of the tumor are identified, a neurosurgeon, a radiation oncologist, and a physicist work together in order to develop the patient's treatment plan.

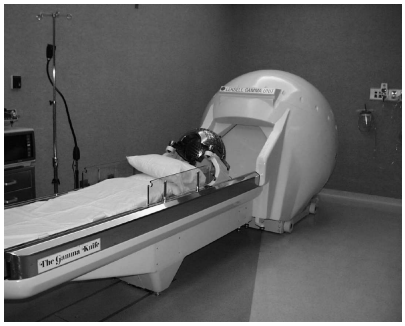

(a) The couch and treatment area

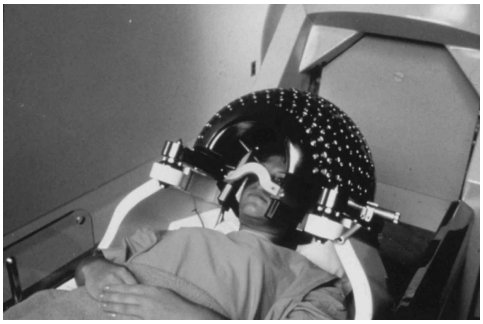

(b) The head-frame and helmet

Figure 1: The Gamma Knife Treatment Unit. A focusing helmet is attached to the frame on the patient's head. The patient lies on the couch and is moved back into the shielded treatment area.

The determination of plans varies substantially in difficulty. For example, some tumors are small enough to require only one shot of radiation. On the other hand, when the shape of the tumor is large or has an irregular shape or is close to a sensitive structure, many shots of different sizes could be needed to achieve a high dose of radiation to the intracranial target volume while sparing the surrounding tissue. Further description of the treatment process, along with some more explanatory figures can be found in [19].

A number of researchers have studied techniques for automating the Gamma Knife treatment planning process. One approach incorporates the assumption that each shot of radiation can be modeled as a sphere. The problem is then reduced to one of geometric coverage, and a ball packing approach [42, 41, 49, 48, 47] can be used to determine the shot locations and sizes. The use of a modified Powell's method in conjunction with simulated annealing has also been proposed [31, 52]. A mixed integer programming (MIP) and a nonlinear programming approach for the problem are presented in [17, 18, 19, 37, 39].

In the model we propose, there are three types of decision variables:

1. *A set of coordinates* (x_s, y_s, z_s): the position of each shot's center is a continuous variable to be chosen. We assume that $\mathcal{S} = \{1, 2, \cdots, m\}$ denotes the set of m shots to be considered in the optimization. Normally, we have to choose $n < m$ of these shots to be used.

2. *A discrete set of collimator sizes*: There are four focusing helmets

available that generate different width shots.

$$\mathcal{W} = \{4mm, 8mm, 14mm, 18mm\}$$

denotes the choices of discrete widths that are available.

3. *Radiation exposure time*: $t_{s,w}$ is the time each shot (s, w) is exposed. It is known that the total dose delivered is a linear function of the exposure time.

The dose delivered at a voxel (i, j, k) in unit time from a shot centered at (x_s, y_s, z_s) can be modeled by a nonlinear function $D_w(x_s, y_s, z_s, i, j, k)$ [11, 25, 43]. The total dose delivered to a voxel (i, j, k) from a given set of shots can then be calculated as

$$Dose(i, j, k) = \sum_{(s,w)\in\mathcal{S}\times\mathcal{W}} t_{s,w} D_w(x_s, y_s, z_s, i, j, k). \tag{3}$$

For each value of $w \in \mathcal{W}$, we use the following functional form

$$D_w(x_s, y_s, z_s, i, j, k) = \sum_{p=1}^{2} \lambda_p \left(1 - \text{erf}\left(\frac{\sqrt{(i-x_s)^2 + \mu_p^y (j-y_s)^2 + \mu_p^z (k-z_s)^2} - r_p}{\sigma_p}\right)\right)$$

to fit the ten parameters λ_p, μ_p^y, μ_p^z, r_p and σ_p to observed data via least-squares. The notation $\text{erf}(x)$ represents the integral of the standard normal distribution from $-\infty$ to x.

In many cases, the planner wishes to limit the use of certain resources. In the Gamma Knife case, there is a bound of n shots, and each shot must have a specified width. If we introduce a binary variable $\psi_{s,w}$ that indicates whether shot s uses width w or not, the following constraints implement the above requirement:

$$\begin{array}{c} 0 \le t_{s,w} \le \psi_{s,w} \bar{t} \\ \sum_{(s,w)\in\mathcal{S}\times\mathcal{W}} \psi_{s,w} \le n. \end{array} \tag{4}$$

Note that the planner needs to specify an upper bound $\bar{t}$ on the exposure time of any shot. The typical range of values for n is $1 - 15$.

It is easy to specify homogeneity in models simply by imposing lower and upper bounds on the dose delivered to voxels in the target $\mathcal{T}$. Similar bounding techniques can be used for avoidance requirements. The imposition of rigid bounds typically leads to plans that are too homogeneous and

not conformal enough, that is, they provide too much dose outside the target. To overcome this problem, the notion of "underdose" was suggested in [18]:

$$Underdose(i,j,k) := \max\{0, \theta - Dose(i,j,k)\}.$$

Informally, underdose measures how much the delivered dose is below the prescribed dose, θ, on the target voxels. Provided we minimize $Underdose$ we can implement this construct using linear constraints:

$$\begin{aligned} \theta &\leq Underdose(i,j,k) + Dose(i,j,k) \\ 0 &\leq Underdose(i,j,k). \end{aligned} \tag{5}$$

The basic model attempts to minimize the underdose subject to the aforementioned constraints on conformity, homogeneity and avoidance.

$$\begin{aligned} \min \quad & \sum_{(i,j,k)\in\mathcal{T}} Underdose(i,j,k) \\ \text{subject to} \quad & (3) \text{ dose definition} \\ & (5) \text{ underdose enforcement constraints} \\ & (2) \text{ conformity constraints} \\ & (1) \text{ dose volume histogram constraints} \\ & (4) \text{ resource use constraints} \\ & x_s, y_s, z_s, t_{s,w} \in \mathbf{R} \\ & 0 \leq Dose(i,j,k) \leq U, \quad \forall (i,j,k) \in \mathcal{T} \\ & \psi_{s,w},\ Exceed(i,j,k) \in \{0,1\} \end{aligned} \tag{6}$$

This model is a nonlinear, mixed integer programming problem. If we choose a fixed set of shot locations (x_s, y_s, z_s) then the model becomes a linear mixed integer programming problem with a collection $(4m)$ of large data matrices $D^s_w(i,j,k)$ replacing the nonlinear functions $D_w(x_s, y_s, z_s, i, j, k)$ in (3). Our investigations found such approaches to be impractical and not as accurate as the scheme outlined below. For realistic instances, the data and number of binary variables becomes very large and the models are unsolvable within the available time limit. Furthermore, the solution quality requires the shot centers to be determined accurately. We therefore resort to methods that include the shot center locations as variables. Similar issues arise in the brachytherapy application we describe later, and we outline a different approach for the solution of that problem.

To avoid the combinatorial issues associated with $\psi_{s,w}$ we use a smooth nonlinear approximation H_α to the step function:

$$H_\alpha(t) := \tfrac{2\arctan(\alpha t)}{\pi}.$$

For increasing values of α, H_α becomes a closer approximation to the step function for $t \geq 0$. We replace (4) with

$$n = \sum_{(s,w)\in\mathcal{S}\times\mathcal{W}} H_\alpha(t_{s,w}). \tag{7}$$

To reduce the number of voxels considered we use a coarse grid $\mathcal{G}$ of voxels in the critical regions and refine the grid appropriately as the calculations progress. To avoid the problems associated with calculating the dose at every voxel in the volume, we approximate the total dose to the volume using

$$\sum_{(s,w)\in\mathcal{S}\times\mathcal{W}} \bar{D}_w t_{s,w} \quad ,$$

where $\bar{D}_w$ is the (measured) dose delivered by a shot of size w to a "phantom". The quantities can be determined once, and used to generate a very good estimate of the total dose delivered to the volume without performing any dose calculations outside the target and the critical organ regions. This leads to the following approximation to the conformity constraint (2):

$$C \sum_{(s,w)\in\mathcal{S}\times\mathcal{W}} \bar{D}_w t_{s,w} \leq \frac{\mathcal{N}_\mathcal{T}}{\mathcal{N}_{\mathcal{G}\cap\mathcal{T}}} \sum_{(i,j,k)\in\mathcal{G}\cap\mathcal{T}} Dose(i,j,k), \tag{8}$$

where $\mathcal{N}.$ represents the number of voxels in the given volume.

Thus, the nonlinear programming model that we use to approximate the solution of (6) has the following form:

$$\begin{array}{ll} \min & \displaystyle\sum_{(i,j,k)\in\mathcal{G}\cap\mathcal{T}} Underdose(i,j,k) \\ \text{subject to} & (3) \text{ dose definition} \\ & (5) \text{ underdose enforcement constraints} \\ & (8) \text{ approximated conformity constraints} \\ & (7) \text{ approximated resource use constraints} \\ & x_s, y_s, z_s, t_{s,w} \in \mathbf{R} \\ & 0 \leq Dose(i,j,k) \leq U, \quad \forall (i,j,k) \in \mathcal{G}\cap\mathcal{T} \\ & 0 \leq t_{s,w} \leq \bar{t} \end{array} \tag{9}$$

A series of five optimization problems are solved to determine the treatment plan. The model is solved iteratively (steps 2, 3, and 4 below) to reduce the total time to find the solution. Our experience shows that combining those three steps into one takes at least three times longer to converge, which is often not clinically acceptable.

1. Conformity estimation. In order to avoid calculating dose outside of the target, we first solve an optimization problem on the target to estimate an "ideal" conformity for the particular patient for a given number of shots. The conformity estimate C is passed to the basic model as an input parameter. Details can be found in [17].

2. Coarse grid estimate. Given the estimate of conformity C, we then specify a series of optimization problems whose purpose is to minimize the total underdose on the target for the given conformity. In order to reduce the computational time required to determine the plan, we first solve (9) on a coarse grid subset of the target voxels. We have found it beneficial to use one or two more shot locations in the model than the number requested by the user, that is $\mathcal{S} := \{1, ..., n + 2\}$, to allow the optimization to choose not only useful sizes but also to discard the extraneous shot locations.

3. Refined grid estimate. To keep the number of voxels in the optimization as small as possible, we only add to the coarse grid those voxels on a finer grid for which the homogeneity (bound) constraints are violated. This procedure improves the quality of the plan without greatly increasing the execution time.

4. Shot reduction problem. In the solution steps given above, we use a small value of α, typically 6 to impose the constraint (7) in an approximate manner. In the fourth solve, we increase the value of α to 100 in an attempt to force the planning system to choose which size/location pairs to use. At the end of this solve, there may still exist some size/location pairs that have very small exposure times t. Also note that our solution technique does not guarantee that the shots are centered at locations within the target.

5. Fixed location model. The computed solution may have more shots used than the user requested and furthermore may not be implementable on the Gamma Knife since the coordinate locations cannot be keyed into the machine. Our approach to adjust the optimization solution to generate implementable coordinates for the shot locations is to round the shot location values and then fix them. Once these locations are fixed, the problem becomes linear in the intensity values t. We reoptimize using (6) and force the user requested number of size/location pairs precisely using a mixed integer program solver.

Note that the starting point for each of the models is the solution point of the previous model. Details on how to generate an effective starting point for the first model are given in [17]. All the optimization models are written using the General Algebraic Modeling System (GAMS) [9] and solved using CONOPT [12] or CPLEX [23].

A subset of the large number of holes in the focusing helmet can be blocked in order to (locally) reduce the amount of radiation delivered or to change the shape of the shot. By determining the amount of radiation that each blocked hole removes and updating D_w appropriately, an extension of the mixed integer model above can be used to further enhance the treatment plan, and spare sensitive structures even more. The "block or not" decision can be modeled using the approach outlined in (4), but this has yet to be implemented in practice due to concerns from clinicians regarding the chances of errors in the physical delivery process.

3 Brachytherapy Treatment Planning

Brachytherapy involves the use of radioactive sources such as catheters or pellets (the latter are referred to as "seeds" below) that are placed within or close to the tumor. A disease site that has been receiving a great deal of attention for conformal treatment planning in brachytherapy is the prostate. The number of diagnosed prostate cancer cases has increased due to the widespread use of the PSA (prostate specific antigen) test. An option for treating prostate cancer is permanent radioactive implant brachytherapy under ultrasound guidance (that is, using needles for injection, the radioactive seeds are permanently implanted in the prostate). While image-guided 3-D conformal treatment planning in brachytherapy is still in its infancy, ultrasound-guided implantation of the prostate is one of the fastest growing medical procedures in the country. The number of such implants is projected to increase to over 100,000 by the year 2005 [2].

In contrast to the Gamma Knife model of the preceding section, the radiation delivery variables for the brachytherapy model consist of only binary variables $Seed(r, s, t)$ that take the value 1 if a seed is placed in voxel (r, s, t) and 0 otherwise (note that seeds may only be placed within the target $\mathcal{T}$). For each possible seed position (r, s, t), a nonlinear dose function (essentially modeling an inverse square law) may then be used to compute a matrix $D_{r,s,t}$ of corresponding radiation doses for all voxels in the region of interest. (Note that the entries of this matrix need only be computed once from the nonlinear radiation function, since translations of this matrix will

yield dose matrices for other seed positions.) The total dose at voxel (i, j, k) is then given as the weighted sum of dose contributions to (i, j, k) from all seeds:

$$Dose(i, j, k) = \sum_{(r,s,t)\in\mathcal{T}} D_{r,s,t}(i, j, k) * Seed(r, s, t). \tag{10}$$

The brachytherapy model also includes non-negative continuous underdose variables as defined in (5) for the target, as well as bounded non-negative overdose variables for each voxel in each organ at risk (OAR):

$$\begin{array}{c} Dose(i, j, k) - Overdose(i, j, k) \leq U_{OAR} \\ 0 \leq Overdose(i, j, k) \leq M - U_{OAR} \end{array} \tag{11}$$

These relations place both soft and hard constraints on the doses to the urethra and rectum. For I-125 implants the urethral and rectal threshold doses U_{OAR} are set to 217.5 Gy and 101.5 Gy respectively. For I-125 the upper dose limits M are set at 275 Gy and 145 Gy for the urethra and rectum respectively by imposing the appropriate upper bounds on the overdose variables.

Finally, the model contains binary variables $Needle(i, j)$ that are forced to have value 1 if a seed is placed at position (i, j) in any plane k:

$$Seed(i, j, k) \quad \leq \quad Needle(i, j). \tag{12}$$

These needle constraints model the mechanics of the implantation process in which a template is used to position the seed-carrying needles and a needle in position (i, j) in the template can then implant seeds in position (i, j) in several different planes k. Since it is undesirable to use a large number of needles, a resource use term representing a weighted sum of $Needle$ variables is used in the objective.

The overall model that we would like to solve then becomes:

$$\begin{array}{lll} \min & \alpha * \displaystyle\sum_{(i,j,k)\in\mathcal{T}} Underdose(i, j, k) + \beta * \sum_{(i,j,k)\in OAR} Overdose(i, j, k) & \\ & +\gamma * \displaystyle\sum_{(i,j)\in template} Needle(i, j) & \\ \text{subject to} & (10) \text{ dose definition} & (13) \\ & (5) \text{ underdose constraints, } (11) \text{ overdose constraints} & \\ & (12) \text{ needle use constraints} & \\ & Seed(i, j, k),\ Needle(i, j) \in \{0, 1\} & \end{array}$$

where α, β, γ are appropriately chosen weights.

Since this model involves so many variables, it is impractical to solve it as a single MIP. Thus, we consider a collection of problems instead, each of which focuses on a subset of variables and constraints that essentially reflects seed implant decisions for a single plane k, assuming that some radiation is already delivered to the voxels in plane k from seeds in the other planes. We use the term "sequential optimization" for this process of cycling through the planes one at a time, adjusting seed placement to optimize incremental doses only in the plane currently under consideration (see [16] for details, and for an alternative MIP based on coarse grids see [30]). For a fixed value of the plane index k we thus need only the pair (i, j) to represent a voxel, and incremental dose within a plane is modeled by replacing the dose equation (10) by

$$Dose(i,j) = InterplaneDose(i,j) + \sum_{(r,s)\in\mathcal{T}_k} D_{r,s,k}(i,j,k) * Seed(r,s,k), \quad (14)$$

where $InterplaneDose(i,j)$ represents the dose contributed to voxel (i,j,k) from seeds in the other planes (as seed positions are changed, these dose contributions are updated) and $\mathcal{T}_k$ is the subset of the target in plane k. Another change needed in the overall model during application of the sequential approach is to update the needle constraints to account for needle positions already in use in the other planes (so that no constraint or corresponding objective function penalty is imposed for those template positions already used in other planes). This simply requires a change in index sets. Since the optimization is performed in sequential plane-by-plane manner, it cannot accurately account for inter-plane variations in the location of the urethra. The urethra is 3-dimensional and shows significant curvature. Poor placement of the seeds in one plane may adversely affect the urethra in other planes. To circumvent this problem, it is possible to add a small number of additional constraints to a 2-D problem to reflect critical structures in nearby planes. Details of this process may be found in [13]. These constraints are termed positioning constraints. The net effect of these constraints is that seeds are less likely to be placed in close proximity to the urethra thereby also reducing the risk of significant impact on the dose distribution to the critical structures in the event that the seeds are misplaced.

Sequential optimization for brachytherapy at the initial pre-plan stage using mixed-integer programming and branch-and-bound has been previously discussed [16]. In that research, the initial values of $InterplaneDose(i,j)$ were based on estimated contributions from other planes, whereas here we

describe the method as modified for operating room (OR) based treatment planning, in which the initial values of $InterplaneDose(i, j)$ are based on seed placements from the pre-plan. Our approach is also based on the premise that the volume of the prostate (target) does not change significantly (more than 5%) between the initial volume study performed weeks before and the actual implant, and this is generally the case for early stage (T1-T2) patients. This allows us to "hot start" the solution process not only by starting with seed placements from the pre-plan, but also provides for faster solutions by limiting seed placement deviations relative to that pre-plan.

Prior to the start of the optimization process, the locations of seeds obtained from the pre-treatment plan are reproduced in the new ultrasound image data set. During optimization, we consider the dose contribution from seeds in other planes up to a distance of 4 cm from the current plane under consideration. Contributions from seeds at a distance greater than 4 cm is negligible [16]. Optimization starts with the outermost planes on each side of the central plane, and proceeding toward the center planes from alternating directions. We found this ordering to be desirable because the small size of the outermost planes implies that there are few possible seed positions, and in some cases it was difficult to deal with these planes once the seed positions in the other slices had been fixed. We also inhibit the introduction of extra needles by increasing the weight γ on the number of needles in the objective function as additional planes are optimized.

The optimization process itself is carried out using GAMS [9] and the commercial mixed-integer programming branch-and-bound solver CPLEX [23]. Using this software, solutions with a relative gap (the gap between the best feasible solution generated and the lower bound of the relaxed mixed-integer programming problem) of $< 1\%$ were obtained in all of the 2-D problems.

In this research, data from 10 patients was used to test this re-optimization framework. Below we consider only those 7 patients receiving radioactive iodine implants (see [13] for data on the additional patients, who received palladium implants, for whom a slightly different analysis is needed). The dose distributions from the pre-treatment (both optimized and manual) plans for the original contours were applied to the new set of contours. These dose distributions were then compared with the dose distribution obtained from the re-optimized plans.

The sequential re-optimization process in the OR can be executed in a single iteration (sweep through all 2-D planar sections) with very good results. Since the pre-treatment optimized plans generally result in loss

Patient #	Pre-man. (%)	Pre-opt. (%)	OR re-opt. (%)	seeds (av.)	needles (av)
1	97.4	94.5	95.3	101	24
2	92.5	95.5	97.2	104	24
3	90.4	93.3	94.8	102	24
4	95.2	93.6	97.0	100	22
5	96.1	93.8	94.7	79	18
6	91.7	92.7	93.3	102	27
7	93.7	95.2	95.2	102	26

Table 1: Target coverage of manual pre-plan vs optimized pre-plan vs OR re-optimized plan

of target coverage when applied to the OR contours, one of the goals of re-optimizing the pre-treatment optimized plan is increasing (recovering) target coverage. At the same time, it is imperative that while achieving this end, no unnecessary deterioration in the dose distribution to the critical structures should occur. Although no undesirable dose increases were observed for the urethra and rectum from the application of the pre-treatment plan to the simulated OR contours, a significant improvement in the dose distribution to the critical structures is achieved by re-optimizing. When compared with the pre-treatment optimized plan, the volume of the rectum exceeding the threshold of 101.5 Gy is reduced in most patients. In the other patients, the increase in this volume is $< 4\%$ and the overdose fraction remains under 20%. In cases in which the dose to the critical structures increases by re-optimizing the pre-treatment optimized plan, this increase is counter-balanced by the increase in target coverage.

The table below provides a partial comparison between pre-plan and re-optimization results. Note that the OR plan always achieves at least 93% target coverage, and in those cases in which this does not represent an improvement relative to both pre-plan results, the re-optimization provides a significant improvement to the OAR dose (see [13] for additional tables of results and DVH plots that give data for the urethra and rectum). For example, for patient 1, the urethra overdose volume fraction is 15% for the both pre-plans and 0% for the re-optimized plan. Note also the average (over all three plans) counts for seeds and needles for each patient, which provide insights into the complexity of treatment planning (seed and needle counts do not vary significantly in the three plans).

Figure 3 shows the difference between the target underdoses for the pre-treatment optimized and re-optimized OR plans for the base and apex planes in the prostate for a representative patient (patient 3). The difference between the plans is most pronounced in these planes. The underdoses (cold spots) would be significant if the pre-treatment plan was used on the day of the procedure. It can be seen from the figure that the re-optimized plan is highly conformal and that significant cold spots are eliminated.

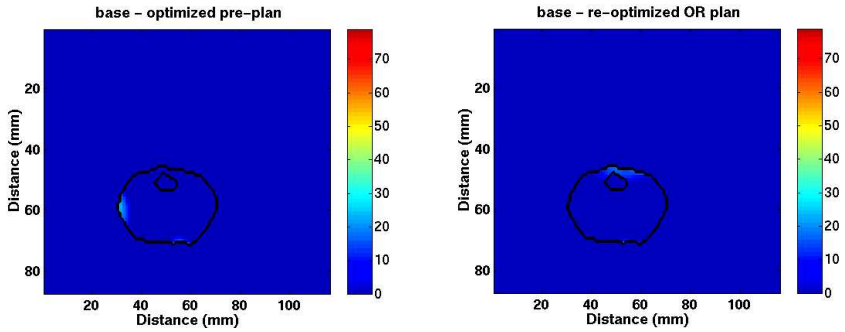

(a) base - pre-plan

(b) base - re-optimized plan

(c) apex - pre-plan

(d) apex - re-optimized plan

Figure 2: Underdose of target regions for (a), (c) the pre-treatment plan and (b), (d) the re-optimized plan. (a) and (b) show the base plane, while (c) and (d) show the apex plane

.

In summary, treatment planning time in the OR is of great importance. The mixed-integer sequential optimization framework allows the pre-plan

to be used to provide initial estimates of seed positions and hence allows the OR-based plan to be performed in about 1/3 of the pre-plan time (i.e., approximately 4 to 8 minutes using a 440 MHz processor).

For our collection of patient data, re-optimization of the treatment plan using simulated OR contours resulted in an increase in target coverage relative to the optimized pre-plan in all cases (maximum increase was 3.4%). Critical structure dose distribution was also improved appreciably. We also found that the addition of positioning constraints to the basic optimization model produced treatment plans that are more robust with respect to possible seed misplacement (simulated by small random displacements) in the OR.

4 IMRT

Intensity modulated radiation therapy (IMRT) represents a rather sophisticated approach in which each radiation treatment (out of a total of perhaps 10-45 such treatments for a patient) involves the application of intensity-modulated beams of radiation from 5-9 different angles (relative to the patient) [4, 6, 8, 35, 44, 45, 46, 51]. The 10X10 centimeter beam cross-section consists of a grid of 100 or more small beamlets of radiation. Intensity modulation is usually accomplished via repeated adjustments of a multileaf collimator (a beam blocking mechanism comprising 40 opposing pairs of tungsten strips or leaves) in which the positions of beam-blocking tungsten leaves are set to allow the passage of radiation for a specified amount of time only in those positions corresponding to the desired beamlets. From an algebraic viewpoint, these binary radiation patterns are weighted by radiation intensities (determined by the length of time radiation is emitted) and the resulting weighted patterns are added together to produce the desired intensity matrix for each angle. This fine level of control of the radiation yields optimization models involving the choice of beam angles and beamlet intensities.

At least two types of optimization problems arise in IMRT treatment planning. The first is the intensity matching problem, and the second is the overall treatment planning problem described above. In the intensity matching problem, a desired integer matrix of beamlet intensities is specified for a given beam angle, and this matrix must be optimally decomposed into an intensity-weighted sum of binary shape matrices representing beamlet patterns that are realizable via potential leaf positions in the collimator. (There are a number of types of IMRT devices currently in clinical use, each

of which has slightly different physical constraints that determine the leaf positions that are possible for that device.)

A simple model for an intensity matching problem is

$$\begin{array}{rl} \min & f(t,c) \\ \text{subject to} & \sum_k t_k * S_k = I, \quad 0 \le t \le Mc \\ & c_k \in \{0,1\}, \end{array} \tag{15}$$

where I is the given integer intensity map matrix, the S_k are realizable binary shape matrices, t_k is a non-negative variable corresponding to the radiation intensity (determined by beam-on time and bounded above by M) associated with shape S_k, and c_k is a binary "shape counter" variable that is forced to 1 if shape S_k is used (which is equivalent to $t_k > 0$). A variety of objective functions f (all of which deal with treatment time and complexity) have been considered for the intensity matching problem, and we describe some of these alternatives after providing some additional background about this problem. Although this formulation has the advantage of simplicity, it is impractical because of the enormous number of shapes S_k.

The intensity matching problem is of critical importance because existing treatment planning software often produces plans that are clinically unacceptable because they require too many changes in the leaf positions at a beam angle. For example, on some equipment the set-up time required to recycle accelerator power (which must be done at each change in leaf positions) is about 7 seconds, so a plan involving 50 leaf positions at each of 9 beam angles (a not uncommon occurrence) would translate into a total treatment time of about one hour, which is clinically undesirable because of patient motion/discomfort problems and because of the need to treat large numbers of patients on a daily basis. (There are other accelerators with much smaller recycle times for which such a complex treatment plan would result in a more acceptable 30 minute or less treatment time, but would still be undesirable since the plan would produce unnecessary wear on the equipment (relative to plans with fewer leaf adjustments) and less accuracy in the delivery of radiation therapy). Langer [28] develops a different formulation based on leaf position variables and considers two objectives: beam-on-time ($f(t,c) = \sum_k t_k$) and cardinality ($f(t,c) = \sum_k c_k$). He circumvents the difficulty of enumerating shape matrices by using binary variables $l(i,j,k)$ and $r(i,j,k)$ corresponding to coverage of bixel (for beam pixel, or position in the shape matrix) (i,j) in shape k by portions of left and right leaves respectively. The continuity of the left leaf in row i in shape k is then enforced by constraints of the form $l(i,j,k) \ge l(i,j+1,k)$ and analogous constraints ap-

ply to the right leaves. (These binary variables may also be used to enforce additional constraints known as "tongue and groove" constraints that relate to adjacent bixels and, for certain types of IMRT machines, "leaf collision" constraints that disallow overlap of left and right leaves in adjacent rows.) Finally, the following constraint guarantees that each bixel is either open to deliver radiation or covered by a leaf: $l(i,j,k)+r(i,j,k)+b(i,j,k) = 1$, where $b(i,j,k)$ is a binary variable that assumes value 1 if radiation is delivered through position (i,j) for a unit time interval. Intensity match corresponds to the constraints

$$\sum_k b(i,j,k) = I(i,j) \quad \forall (i,j). \tag{16}$$

To deal with the minimum cardinality problem in which the number of shapes is minimized ($f(t,c) = \sum_k c_k$), the binary shape change variable c_k is subjected to the constraints $-c_k \leq b(i,j,k) - b(i,j,k+1) \leq c_k$, forcing it to 1 if any bixel changes from open to covered or vice-versa in the transition from time period k to time period $k+1$. Since large system of constraints must be constructed for every time interval (that is, the range of k is at least as long as the total treatment time), this approach gives rise to very large constraint sets, but has been effective for problems in which the intensity maps are not very complex.

An interesting shortest path approach to the intensity matching problem has been developed recently by Boland, et al. [3]. They consider the easier (from an optimization viewpoint) objective of minimizing total beam-on time ($f(t,c) = \sum_k t_k$) and show that optimal solutions can be obtained very quickly by solving a problem in a graph with certain side constraints. Boland, et al. avoid the replication of constraint systems by constructing a layered graph whose nodes represents possible pairs of left/right leaf positions for each successive row, and whose arcs represent allowable transitions to the leaf pairs in the next row (leaf collision constraints are enforced by excluding certain arcs). They then observe that a path from the top row to the bottom row in this graph corresponds to an allowable shape. The variables are the flows on these paths, which correspond to intensity variables for the left/right row segments. Side constraints are used to ensure intensity match. By considering conformal decomposition of the flows into paths, it is easy to see that minimizing total flow from sources to sinks is equivalent to minimizing beam-on time. The resulting problem is a linear program that can usually be solved in under a minute with good LP software. However, this approach does not extend readily to the minimum cardinality case, because the graph model is based on flows and the cardinality problem would require

a count of the number of paths used. Thus, there are clearly opportunities for further research in this area, since Langer observes from his numerical results that minimal beam-on time solutions may have relatively large cardinality. Column generation approaches that approximate the problem [34] may be promising in this regard.

The IMRT treatment planning problem at the bixel level may be defined in terms of intensity variables $I(r,s,a)$ where (r,s) are bixel indices and a is a beam angle index and $D_{r,s,a}(i,j,k)$ is the dose at (i,j,k) resulting from a unit value of the integer variable $I(r,s,a)$. The resulting model is similar to the brachytherapy model in that the dose definition is given by:

$$Dose(i,j,k) = \sum_{(r,s,a)} D_{r,s,a}(i,j,k) * I(r,s,a). \tag{17}$$

The optimization model may now be stated as:

$$\begin{array}{ll} \min & \alpha * \sum_{(i,j,k)\in\mathcal{T}} Underdose(i,j,k) + \beta * \sum_{(i,j,k)\in OAR} Overdose(i,j,k) \\ \text{subject to} & (17) \text{ dose definition} \\ & (5) \text{ underdose constraints} \\ & (11) \text{ overdose constraints} \\ & I(r,s,a) \text{ integer.} \end{array} \tag{18}$$

Key difficulties with this model in addition to its overall size and number of integer variables include choosing promising beam angles. Note that a solution of this model will result in bixel intensity maps (for each shot angle), and these must then be decomposed via solutions of intensity matching problems in order to obtain the final treatment plan. New techniques for the full IMRT treatment planning problem have been proposed in [40] (using simulated annealing) and [34] (using column generation). Possibilities for future research include slicing approaches analogous to those that we have previously successfully employed for brachytherapy [14, 15]. In the slicing approach, radiation delivery would be optimized for a selected beam angle, assuming a certain total amount of radiation to tissues from the remaining beam angles, and then this optimization procedure would be repeated one beam angle at a time for a promising list of beam angles. The slicing approach has the advantage of significantly reducing the size of the optimization problems considered, but requires the construction of a good set of initial conditions, including a good priority list for beam angles. Ongoing work is focusing on methodology to rank beam angle suitability for a given

treatment. Nested partitions [26] may also be useful in this context in terms of providing a structured approach for stochastically sampling the space of beam angles and shape matrices.

5 Conclusions and Directions for Future Research

The large-scale combinatorial problems arising from radiation treatment planning offer significant challenges to the optimization community because they contain large numbers of variables and constraints as well as large amounts of data. We have shown here that carefully tailored optimization approaches that approach the "ideal" version of treatment planning problems through a series of simpler problems and "hot starts" can yield high-quality treatment plans in areas of both teletherapy and brachytherapy. However, there remain many open problems because of the diversity and ever increasing complexity of radiation delivery mechanisms. In particular, treatment planning problems arising in intensity modulated radiation therapy represent an extremely complex class of optimization problems for which fast techniques that provide results of guaranteed quality are currently needed. Given the critical importance of utilizing radiation technology in a manner that maximizes tumor control and minimizes harmful radiation to the patient, and the impracticality of dealing with this complex technology by trial-and-error, we are confident that researchers in optimization will be able to develop the effective new software tools that are needed.

References

[1] G. Arcangeli, M. Benassi, L. Nieddu, C. Passi, G. Patrizi, and M.T. Russo. Optimal adaptive control of treatment planning in radiation therapy. *European Journal of Operational Research*, 140:399–412, 2002.

[2] BBIN. *Biomedical Business International Newsletter*, pages 72–75, 1996.

[3] N. Boland, H.W. Hamacher, and F. Lenzen. Minimizing beam-on time in cancer radiation treatment using multileaf collimators. Report wirtschaftsmathematik, Department of Mathematics, University Kaiserslautern, 2002.

[4] T. R. Bortfeld, D. L. Kahler, T. J. Waldron, and A. L. Boyer. X-ray field compensation with multileaf collimators. *International Journal of Radiation Oncology, Biology and Physics*, 28(3):723–730, 1994.

[5] A. Brahme. Biological and physical dose optimization in radiation therapy. In J.G. Fortner and J.E. Rhoads, editors, *Accomplishments in Cancer Research*, pages 265–298. General Motors Cancer Research Foundation, 1991.

[6] A. Brahme. Optimization of radiation therapy and the development of multileaf collimation. *International Journal of Radiation Oncology, Biology and Physics*, 25:373–375, 1993.

[7] A. Brahme. Treatment optimization: Using physical and radiobiological objective functions. In A. R. Smith, editor, *Radiation Therapy Physics*, pages 209–246. Springer-Verlag, Berlin, 1995.

[8] L. Brewster, R. Mohan, G. Mageras, C. Burman, S. Leibel, and Z. Fuks. Three dimensional conformal treatment planning with multileaf collimators. *International Journal of Radiation Oncology, Biology and Physics*, 33(5):1081–1089, 1995.

[9] A. Brooke, D. Kendrick, and A. Meeraus. *GAMS: A User's Guide*. The Scientific Press, South San Francisco, California, 1988.

[10] Yair Censor. Parallel application of block-iterative methods in medical imaging and radiation therapy. *Mathematical Programming*, 42:307–325, 1988.

[11] P. S. Cho, H. G. Kuterdem, and R. J. Marks. A spherical dose model for radiosurgery treatment planning. *Physics in Medicine and Biology*, 43:3145–3148, 1998.

[12] A. Drud. CONOPT: A GRG code for large sparse dynamic nonlinear optimization problems. *Mathematical Programming*, 31:153–191, 1985.

[13] W. D. D'Souza and R. R. Meyer. An intraoperative reoptimization framework for prostate implant treatment plans. Technical report, Computer Sciences Department, University of Wisconsin-Madison, in preparation 2002.

[14] W. D. D'Souza, R. R. Meyer, M. C. Ferris, and B. R. Thomadsen. Mixed integer programming models for prostate brachytherapy treatment optimization. *Medical Physics*, 26(6):1099, 1999.

[15] W. D. D'Souza, R. R. Meyer, M. C. Ferris, and B. R. Thomadsen. Mip models and bb strategies in brachytherapy treatment optimization. *Journal of Global Optimization, forthcoming*, 2002.

[16] W. D. D'Souza, R. R. Meyer, B. R. Thomadsen, and M. C. Ferris. An iterative sequential mixed-integer approach to automated prostate brachytherapy treatment optimization. *Physics in Medicine and Biology*, 46:297–322, 2001.

[17] M. C. Ferris, J.-H. Lim, and D. M. Shepard. Optimization approaches for treatment planning on a Gamma Knife. *SIAM Journal on Optimization, forthcoming*, 2002.

[18] M. C. Ferris, J.-H. Lim, and D. M. Shepard. Radiosurgery treatment planning via nonlinear programming. *Annals of Operations Research, forthcoming*, 2002.

[19] M. C. Ferris and D. M. Shepard. Optimization of Gamma Knife radiosurgery. In D.-Z. Du, P. Pardalos, and J. Wang, editors, *Discrete Mathematical Problems with Medical Applications*, volume 55 of *DIMACS Series in Discrete Mathematics and Theoretical Computer Science*, pages 27–44. American Mathematical Society, 2000.

[20] M. C. Ferris and M. M. Voelker. Neuro-dynamic programming for radiation treatment planning. Numerical Analysis Group Research Report NA-02/06, Oxford University Computing Laboratory, Oxford University, 2002.

[21] J. C. Ganz. *Gamma Knife Surgery*. Springer-Verlag Wien, Austria, 1997.

[22] H. W. Hamacher and K.-H. Küfer. Inverse radiation therapy planning — a multiple objective optimization approach. *Discrete Applied Mathematics*, 118:145–161, 2002.

[23] ILOG CPLEX Division, 889 Alder Avenue, Incline Village, Nevada. *CPLEX Optimizer*. `http://www.cplex.com/`.

[24] L.C. Jones and P.W. Hoban. Treatment plan comparison using equivalent uniform biologically effective dose (EUBED). *Physics in Medicine and Biology*, pages 159–170, 2000.

[25] H. M. Kooy, L. A. Nedzi, J. S. Loeffler, E. Alexander, C. Cheng, E. Mannarino, E. Holupka, and R. Siddon. Treatment planning for streotactic radiosurgery of intra-cranial lesions. *International Journal of Radiation Oncology, Biology and Physics*, 21:683–693, 1991.

[26] L. Shi L. and S. Olafsson. Nested partitions method for global optimization. *Operations Research*, 48:390–407, 2000.

[27] M. Langer, S. Morrill, R. Brown, O. Lee, and R. Lane. A comparison of mixed integer programming and fast simulated annealing for optimized beam weights in radiation therapy. *Medical Physics*, 23:957–964, 1996.

[28] M. Langer, V. Thai, and L. Papiez. Improved leaf sequencing reduces segments or monitor units needed to deliver IMRT using multileaf collimators. *Medical Physics*, 28(12):2450–2458, 2001.

[29] E. K. Lee, T. Fox, and I. Crocker. Optimization of radiosurgery treatment planning via mixed integer programming. *Medical Physics*, 27:995–1004, 2000.

[30] E.K. Lee, R.J. Gallagher, D. Silvern, C.S. Wuu, and M. Zaider. Treatment planning for brachytherapy: an integer programming model, two computational approaches and experiments with permanent prostate implant planning. *Physics in Medicine and Biology*, pages 145–165, 1999.

[31] L. Luo, H. Shu, W. Yu, Y. Yan, X. Bao, and Y. Fu. Optimizing computerized treatment planning for the Gamma Knife by source culling. *International Journal of Radiation Oncology, Biology and Physics*, 45(5):1339–1346, 1999.

[32] S. M. Morrill, K. S. Lam, R. G. Lane, M. Langer, and I. I. Rosen. Very fast simulated annealing in radiation therapy treatment plan optimization. *International Journal of Radiation Oncology, Biology and Physics*, 31:179–188, 1995.

[33] A. Niemierko. Radiobiological models of tissue response to radiation in treatment planning systems. *Tumori*, 84:140–143, 1998.

[34] F. Preciado-Walters, R. Rardin, M. Langer, and V. Thai. A coupled column generation, mixed-integer approach to optimal planning of intensity modulated radiation therapy for cancer. Technical report, Industrial Engineering, Purdue University, 2002.

[35] W. Que. Comparison of algorithms for multileaf collimator field segmentation. *Medical Physics*, 26:2390–2396, 1999.

[36] W. Schlegel and A. Mahr, editors. *3D Conformal Radiation Therapy - A Multimedia Introduction to Methods and Techniques*. Springer-Verlag, Berlin, 2001.

[37] D. M. Shepard, L. S. Chin, S. J. DiBiase, S. A. Naqvi, J. Lim, and M. C. Ferris. Clinical implementation of an automated planning system for Gamma Knife radiosurgery. Technical report, University of Maryland School of Medicine, Baltimore, Maryland, 2002. Submitted to International Journal of Radiation Oncology, Biology, Physics.

[38] D. M. Shepard, M. C. Ferris, G. Olivera, and T. R. Mackie. Optimizing the delivery of radiation to cancer patients. *SIAM Review*, 41:721–744, 1999.

[39] D. M. Shepard, M. C. Ferris, R. Ove, and L. Ma. Inverse treatment planning for Gamma Knife radiosurgery. *Medical Physics*, 27:12, 2000.

[40] D.M. Shepard, M.A. Earl, X.A. Li, and C. Yu. Direct aperture optimization: A turnkey solution for step-and-shoot IMRT. *Medical Physics*, 29:1007–1018, 2002.

[41] R. A. Stone, V. Smith, and L. Verhey. Inverse planning for the Gamma Knife. *Medical Physics*, 20:865, 1993.

[42] J. Wang. Packing of unequal spheres and automated radiosurgical treatment planning. *Journal of Combinatorial Optimization*, 3:453–463, 1999.

[43] S Webb. Optimisation of conformal radiotherapy dose distributions by simulated annealing. *Physics in Medicine and Biology*, 34(10):1349–1370, 1989.

[44] S. Webb. Inverse planning for imrt: the role of simulated annealing. In E. Sternick, editor, *The Theory and Practice of Intensity Modulated Radiation Therapy*. Advanced Medical Publishing, 1997.

[45] S. Webb. Configuration options for intensity-modulated radiation therapy usi ng multiple static fields shaped by a multileaf collimator. *Physics in Medicine and Biology*, 43:241–260, 1998.

[46] S. Webb. Configuration options for intensity-modulated radiation therapy using multiple static fields shaped by a multileaf collimator. II: Constraints and limitations on 2D modulation. *Physics in Medicine and Biology*, 43:1481–1495, 1998.

[47] A. Wu, G. Lindner, and A. H. Maitz et al. Physics of gamma knife approach on convergent beams in stereotactic radiosurgery. *International Journal of Radiation Oncology, Biology and Physics*, 18(4):941–949, 1990.

[48] Q. J. Wu. Sphere packing using morphological analysis. In D.-Z. Du, P. Pardalos, and J. Wang, editors, *Discrete Mathematical Problems with Medical Applications*, volume 55 of *DIMACS Series in Discrete Mathematics and Theoretical Computer Science*, pages 45–54. American Mathematical Society, 2000.

[49] Q. J. Wu and J. D. Bourland. Morphology-guided radiosurgery treatment planning and optimization for multiple isocenters. *Medical Physics*, 26(10):2151–2160, 1999.

[50] Q. J. Wu, J. Wang, and C. H. Sibata. Optimization problems in 3D conformal radiation therapy. In D.-Z. Du, P. Pardalos, and J. Wang, editors, *Discrete Mathematical Problems with Medical Applications*, volume 55 of *DIMACS Series in Discrete Mathematics and Theoretical Computer Science*, pages 183–194. American Mathematical Society, 2000.

[51] P. Xia and L.J. Verhey. Multileaf collimator leaf sequencing algorithm for intensity modula ted beams with multiple static segments. *Medical Physics*, 25(8):1424–1434, 1998.

[52] Y. Yan, H. Shu, and X. Bao. Clinical treatment planning optimization by Powell's method for Gamma unit treatment system. *International Journal of Radiation Oncology, Biology and Physics*, 39:247–254, 1997.